

# Numerical evaluation of screening length and anomalous small-angle X-ray scattering of polystyrene in benzene

O. Kube\*, E. Wendt and J. Springer

*Institut für Technische Chemie der Technischen Universität Berlin, Fachgebiet  
Makromolekulare Chemie, Strasse des 17 Juni 135, 1000 Berlin 12, FRG  
(Received 24 July 1986; revised 22 January 1987; accepted 5 March 1987)*

Small-angle X-ray scattering (SAXS) of polystyrene ( $52\,000\text{ g mol}^{-1} \leq M_w \leq 4\,390\,000\text{ g mol}^{-1}$ ,  $14\text{ g l}^{-1} \leq c \leq 201\text{ g l}^{-1}$ ,  $T = 21^\circ\text{C}$ ) in benzene is investigated with a Kratky slit camera. The screening length obtained from desmeared SAXS curves by Zimm plots is compared to values obtained with direct numerical evaluation of the smeared SAXS curves. Good agreement is found. Several SAXS curves exhibit an anomalous rise of intensity at very small angles. The size of the long-range heterogeneities responsible for anomalous SAXS is investigated with numerical methods. Within the accessible error limit the size does not depend on molecular weight or concentration.

(Keywords: X-ray scattering; indirect Fourier transformation; polystyrene; semidilute solutions; screening length; long-range heterogeneities)

## INTRODUCTION

The thermodynamics and structure of chain molecules in solution have been extensively studied<sup>1-4</sup> and an analysis of a measured small-angle X-ray scattering (SAXS) curve can usually be done on the basis of a physical model<sup>1-3</sup>. However, if SAXS measurements are carried out for instance with a Kratky slit camera one has to correct distortions owing to the geometry of the primary beam prior to evaluation<sup>2</sup>.

For standard applications it is therefore desirable to reduce the data evaluation to one step. This can conveniently be done by using a method we will refer to as indirect Fourier transformation (IFT) (see ref. 2, pp. 131-9). In the examples presented the SAXS curves are approximated by a sum of suitable basis functions which allow correction of slit length distortions and further can be analytically Fourier-transformed to real space. From the distance distribution function all desired parameters can be calculated. Though correctness of results obtained by the IFT method can be tested with numerical examples it is desirable to have a practical check of its reliability.

Since the theory of semidilute solutions is experimentally verified<sup>5-8</sup>, experimental conditions are easy to match and results obtained can be compared to those of other authors, measurements of the screening length  $\xi$  (see ref. 3, pp. 76-88, and ref. 5) of semidilute solutions of polystyrene in benzene were carried out. Results obtained by the IFT method were then compared to results obtained by a Zimm plot with desmeared SAXS curves.

One further purpose of these measurements was a rough check of range of molecular weight and range of concentration where anomalous small-angle scattering of polystyrene in benzene<sup>9-11</sup> can be observed by SAXS. Above concentrations when the chains begin to overlap

one observes a strong rise of intensity at very small angles. Well within the semidilute concentration regime there is further experimental evidence for a component with slow diffusional motion detectable by means of inelastic light scattering<sup>12,13</sup>. This component is referred to as particle aggregates and is most probably responsible for anomalous small-angle scattering. Since the nomenclature 'particle aggregates' implies a defined structure, we adopt the more neutral nomenclature 'long-range heterogeneities' (LRH) chosen by Koberstein *et al.*<sup>9</sup> and Gan *et al.*<sup>10</sup>.

## THEORY

In the case of randomly oriented chain molecules in solution one only needs to consider the averaged one-dimensional distance distribution function  $p(r)$ , which will be referred to as the  $p(r)$  function in what follows. The  $p(r)$  function and the appropriately normalized scattered intensity  $I(h)$  are connected by Fourier transformation<sup>2</sup>

$$I(h) = 4\pi \int_0^\infty p(r) \frac{\sin(hr)}{hr} dr \quad (1)$$

where  $h = (4\pi/\lambda) \sin \theta$ ,  $\lambda$  is the wavelength of the radiation,  $2\theta$  the angle between primary beam and scattered radiation,  $r$  the distance between scattering centres and

$$p(r) = \frac{1}{2\pi^2} \int_0^\infty I(h) hr \sin(hr) dh \quad (2)$$

According to de Gennes<sup>3</sup> the  $p(r)$  function in the case of a semidilute solution of identical chains in a good solvent is given by

$$p(r) = \text{constant} \times r \exp(-r/\xi) \quad \xi < r < R_{\text{gyr}} \quad (3)$$

where  $\xi$  is the screening length and  $R_{\text{gyr}}$  the radius of gyration of a single chain. Fourier transformation of

\* Present address: Henkel KGaA, 4000 Düsseldorf, Henkelstr. 67, FRG

equation (3) according to equation (2) yields

$$I(h) = \frac{\text{constant}}{h^2 + \xi^{-2}} \quad \xi^{-1} > h > R_{\text{gyl}}^{-1} \quad (4)$$

Plots of  $I(h)^{-1}$  versus  $h^2$  will be referred to as Zimm plots.

If one assumes the validity of equation (3) over the whole  $r$  range, parameters such as average length  $\langle L \rangle$  and mean square length  $\langle R^2 \rangle$  obtainable from the  $p(r)$  function should be connected to the screening length according to

$$\langle L \rangle = \frac{\int_0^\infty r p(r) dr}{2 \int_0^\infty p(r) dr} = \xi \quad \langle R^2 \rangle = \frac{\int_0^\infty r^2 p(r) dr}{2 \int_0^\infty p(r) dr} = 3\xi^2 \quad (5)$$

The average length and the mean square length are only used in the sense of equation (5) and do not refer to properties of a single chain. Equation (5) will be used to determine the screening length by the IFT method.

It should be noted that the relations given in equation (5) can be used as an implicit check for consistency of  $p(r)$  functions obtained with the IFT method.

Since SAXS measurements are carried out with a Kratky camera, distortions caused by the geometry of the primary beam have to be corrected. For the measured SAXS curves slit length correction is fully sufficient. The measured smeared intensity  $I_{\text{sm}}(h)$  is then related to the desmeared intensity  $I(h)$  by<sup>2</sup>:

$$I_{\text{sm}}(h) = \int_0^{t_{\text{max}}} P(t) I((h^2 + t^2)^{1/2}) dt \quad \int_0^{t_{\text{max}}} P(t) dt = 1 \quad (6)$$

where  $P(t)$  is the length profile of the primary beam, symmetric to  $t = 0 \text{ nm}^{-1}$ , and  $t$  is the coordinate along the length of the primary beam.

#### Numerical data evaluation

For an approximation of the desmeared intensity we use a sum of Gaussian (program GAUSS2) or Lorentzian functions (program LORQ1) respectively:

$$I(h) = \sum_{k=1}^N a_k \exp(-b_k h^2) \quad (7)$$

$$I(h) = \sum_{k=1}^N \frac{a_k}{(b_k^2 + h^2)^2} \quad (8)$$

When smeared according to equation (6), coefficients  $a_k$  and  $b_k$  can be determined by a least-squares fit to the measured SAXS curve. To determine the  $p(r)$  function equations (7) and (8) which extend from 0 to  $\infty$  can be Fourier-transformed analytically according to equation (2). A speciality of the programs used is that one works with a predetermined fixed set of non-linear coefficients  $b_k$ . Since coefficients  $a_k$  should be positive, they are determined by a constrained (non-negative) linear least-squares fit. Contrary to Glatter's approach (ref. 2, pp. 131–9),  $p(r)$  functions obtainable via equations (7) and (8) only resemble band-limited  $p(r)$  functions, but mathematically extend to infinity. Details about the programs have been submitted elsewhere<sup>14</sup>.

#### EXPERIMENTAL

All measurements were carried out with a Kratky camera (model 11000, Anton Paar, Graz, Austria) and filtered (Ni foil) Cu K $\alpha$  X-rays. The X-ray generator was operated at 40 mA and 40 kV. SAXS was measured with a position-

sensitive detector (PSD) (model OED50, M. Braun, Garching, Germany) at distances of 525 or 265 mm from the sample plane. The number of points was numerically reduced afterwards by combining from three to seven channels. A single channel of the PSD refers to an area of  $0.07 \times 5 \text{ mm}^2$ .

In all SAXS curves shown, measured solvent scattering is already subtracted.

Polystyrene samples ( $M_w = 52\,000 \text{ g mol}^{-1}$  and  $M_w = 260\,000 \text{ g mol}^{-1}$ ) were prepared anionically<sup>15,16</sup> and characterized by means of gel permeation chromatography and viscosity. All other polystyrene samples were polymer standards (Knauer, Berlin, Germany, and PSS, Mainz, Germany). All polystyrene samples had a narrow distribution with  $M_w/M_n < 1.2$ . Solutions were prepared at room temperature and allowed to stand at least 2 days prior to measurement. To characterize the semidilute concentration regime the restrictive inequality

$$[\eta]^{-1} \leq c \leq \rho_2 \quad (9)$$

is used, where  $[\eta]$  is the intrinsic viscosity,  $c$  is the concentration and  $\rho_2$  is the bulk density of polymer.

#### RESULTS AND DISCUSSION

##### Screening length

Figure 1 shows SAXS curves of a measured concentration series. For an analysis of the screening length the strong scattering in the very small-angle region of the two highest concentrations will be omitted.

A fit with program GAUSS2 to a measured SAXS curve is shown in Figure 2. The  $p(r)$  functions determined by both programs are shown in Figure 3 for comparison. The undulation at small  $r$  values of the  $p(r)$  function determined with GAUSS2 is an artefact due to the chosen approximating function. When the relation  $r = \pi/h$  is considered it is easily seen that the range  $r < 1 \text{ nm}$  in the  $p(r)$  function corresponds to an extrapolation in  $h$  space. The desmeared SAXS curves obtained from both programs agree almost exactly in the measured range. However, to obtain an unbiased desmeared SAXS curve both curves were averaged. Figure 4 shows a Zimm plot to the averaged desmeared SAXS curve.

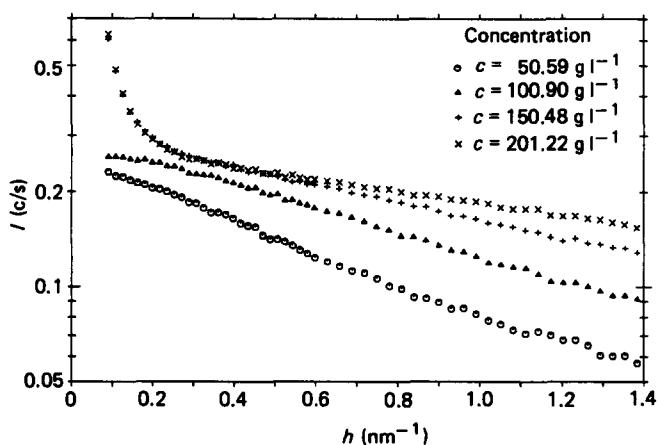


Figure 1 SAXS of a concentration series with anomalous SAXS at  $c = 150.48 \text{ g l}^{-1}$  and  $c = 201.22 \text{ g l}^{-1}$ . Solvent-corrected scattering, PS/BE,  $M_w = 260\,000 \text{ g mol}^{-1}$ ,  $T = 21.0^\circ\text{C}$

Results for all measured samples are shown in Table 1. The results obtained for  $\xi$ ,  $\langle L \rangle$  and  $(\langle R^2 \rangle/3)^{1/2}$  in Table 1 agree reasonably well, demonstrating the reliability of the IFT method. The agreement of  $\langle L \rangle$  and  $(\langle R^2 \rangle/3)^{1/2}$

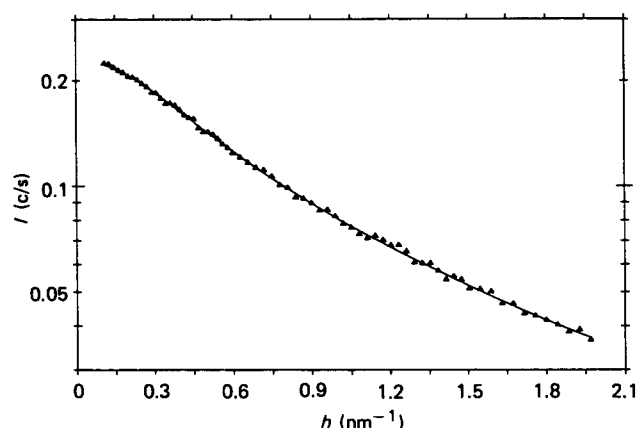


Figure 2 Smeared fit with program GAUSS2 to a measured SAXS curve:  $\Delta$ , measured data; —, fit. PS/BE,  $M_w = 260\,000\text{ g mol}^{-1}$ ,  $c = 50.59\text{ g l}^{-1}$ ,  $T = 21.0^\circ\text{C}$

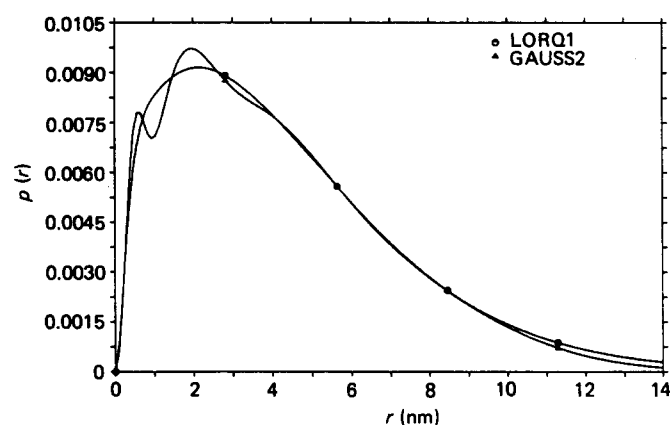


Figure 3 The  $p(r)$  functions obtained with programs GAUSS2 and LORQ1. PS/BE,  $M_w = 260\,000\text{ g mol}^{-1}$ ,  $c = 50.59\text{ g l}^{-1}$ ,  $T = 21.0^\circ\text{C}$

further justifies the lower integration limit used in equation (5).

In the case of anomalous SAXS the innermost data are neglected. The number of points removed is chosen visually.

Figures 5 and 6 show shifted plots of determined quantities  $\xi$ ,  $\langle L \rangle$  and  $(\langle R^2 \rangle/3)^{1/2}$  (Table 1) versus concentration. The calculated coefficients  $k_1$  and  $k_2$  according to

$$\xi = k_1(c/c')^{k_2} \quad (c' = 1\text{ g l}^{-1})$$

are listed in Table 2. For comparison the values obtained by King *et al.*<sup>8</sup> for polystyrene in toluene are included in Table 2. Though within the range of experimental errors, lower values of  $k_1$  and  $k_2$  obtained with both programs for  $(\langle R^2 \rangle/3)^{1/2}$  indicate a systematic deviation.

#### Anomalous SAXS

The physical structure of the long-range heterogeneities responsible for anomalous SAXS is still not clear<sup>9,10</sup>. So it remains to determine amount, average size and if possible dependence on concentration of polystyrene, molecular weight of polystyrene and temperature of the solution<sup>10</sup>.

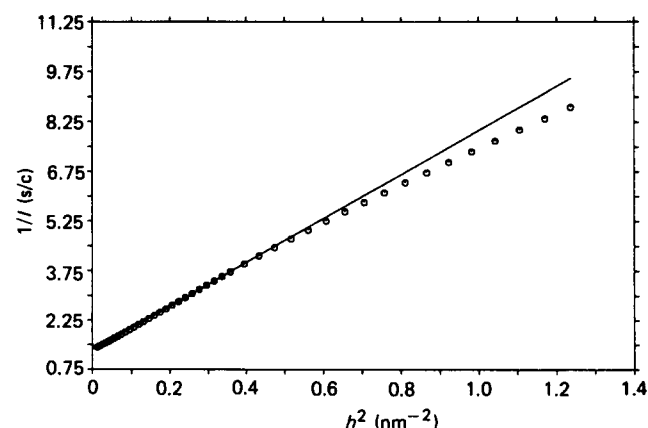


Figure 4 Zimm plot to averaged desmeared SAXS curve. PS/BE,  $M_w = 260\,000\text{ g mol}^{-1}$ ,  $c = 50.59\text{ g l}^{-1}$ ,  $T = 21.0^\circ\text{C}$ ,  $\xi = 2.23\text{ nm}$

Table 1

$M_w$ ( $\text{g mol}^{-1}$ )	$c$ ( $\text{g l}^{-1}$ )	Zimm plot $\xi$ (nm)	GAUSS2		LORQ1	
			$\langle L \rangle$ (nm)	$(\langle R^2 \rangle/3)^{1/2}$ (nm)	$\langle L \rangle$ (nm)	$(\langle R^2 \rangle/3)^{1/2}$ (nm)
52 000	103.24	1.47	1.41	1.38	1.55	1.60
	199.30	0.86	0.85	0.90	0.98	1.14
260 000	50.59	2.23	2.12	2.08	2.23	2.22
	100.90	1.52	1.53	1.53	1.49	1.50
	150.48	1.05	1.09	1.10	1.08	1.10
	201.22	0.88	0.84	0.87	0.92	1.00
480 000	18.03	4.46	4.44	4.24	4.68	4.64
	30.34	3.21	2.67	2.54	3.02	2.98
	45.74	2.47	2.18	2.11	2.78	2.79
	68.60	1.63	1.70	1.72	1.61	1.62
	113.97	0.96	0.92	0.94	0.94	0.96
	174.60	0.80	0.74	0.71	0.82	0.82
600 000	100.00	1.34	1.26	1.23	1.30	1.29
1 460 000	41.10	2.87	2.66	2.54	2.76	2.70
1 800 000	33.50	3.00	2.89	2.76	3.12	3.15
2 510 000	24.00	3.72	3.81	3.66	4.19	4.09
2 950 000	20.40	3.97	4.00	3.84	4.16	4.08
4 390 000	14.00	5.58	5.42	5.10	5.65	5.45

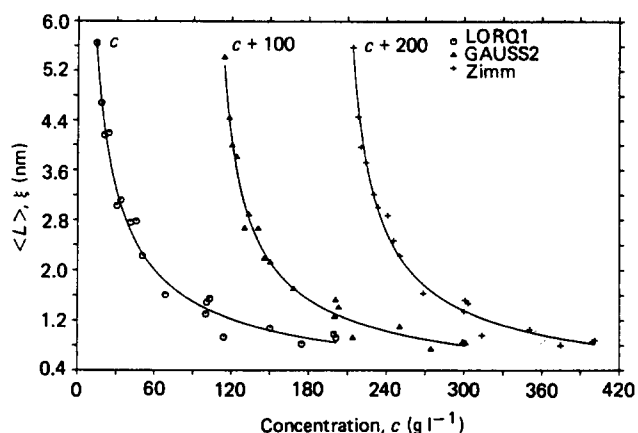


Figure 5  $\langle L \rangle$  (LORQ1, GAUSS2) and  $\xi$  (Zimm plot) versus concentration (see Table 1). Plots are shifted as indicated along the concentration axis

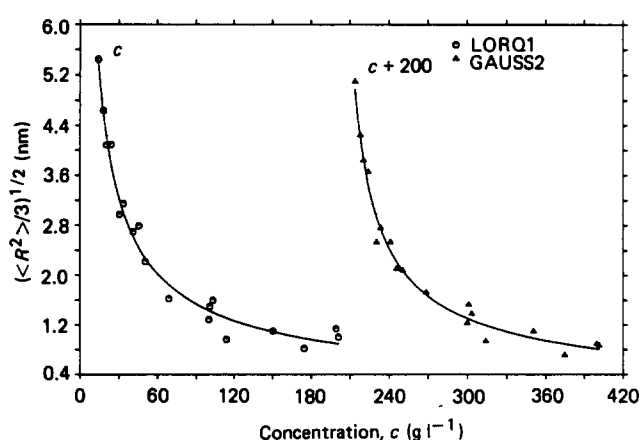


Figure 6  $\langle R^2 \rangle / 3^{1/2}$  (LORQ1, GAUSS2) versus concentration (see Table 1). Plots are shifted as indicated along the concentration axis

Table 2

Method	Quantity	$k_1$ (nm)	$k_2$
Zimm plot	$\xi$	36.5	-0.72
GAUSS2	$\langle L \rangle$	34.6	-0.71
GAUSS2	$\langle R^2 \rangle / 3^{1/2}$	30.1	-0.68
LORQ1	$\langle L \rangle$	37.1	-0.71
LORQ1	$\langle R^2 \rangle / 3^{1/2}$	32.7	-0.68
Zimm plot <sup>8</sup>	$\xi$	36.4	-0.70

The measured concentration series ( $M_w = 260\,000\text{ g mol}^{-1}$ ) in Figure 1 is a typical example for anomalous SAXS. The onset concentration of anomalous SAXS is located between the concentrations  $100.90\text{ g l}^{-1}$  and  $150.48\text{ g l}^{-1}$  ( $M_w = 260\,000\text{ g mol}^{-1}$ ), and anomalous SAXS becomes apparently stronger with higher concentration of polystyrene. Within the series of polystyrene of  $M_w = 480\,000\text{ g mol}^{-1}$  the onset concentration is located between  $68.60\text{ g l}^{-1}$  and  $113.97\text{ g l}^{-1}$ . For polystyrene of  $M_w = 600\,000\text{ g mol}^{-1}$  only one concentration ( $100.00\text{ g l}^{-1}$ ) was measured, but a considerable amount of anomalous SAXS is already present. Owing to strong scattering of molecular weights  $M_w \geq 1\,460\,000\text{ g mol}^{-1}$  no anomalous SAXS could be identified.

Precise evaluation of average size and amount of long-

range heterogeneities from our data, however, is not possible owing to insufficient resolution.

Assuming a band-limited  $p(r)$  function one can, according to the Fourier sampling theorem<sup>17</sup>, accurately restore  $p(r)$  functions up to  $r_{\max} \leq \pi/h_{\min}$ , where  $h_{\min}$  is the lowest  $h$  value measured. The lowest  $h$  value reached in our experiments is  $h_{\min} = 0.053\text{ nm}^{-1}$ , setting an upper limit of  $r_{\max} \leq 59\text{ nm}$ . The long-range heterogeneities largely exceed this value (compare values given for radius in Table 3).

The missing information can only be restored by use of a model, which in turn strongly influences calculated parameters. To obtain a reliable estimate of average size of long-range heterogeneities and range of error, we use four models and average results calculated with them. Additionally to equations (7) and (8) we employ

$$I(h) = \frac{a_1}{(a_2 + h^2)^2} + \frac{a_3}{a_4 + h^2} \quad (10)$$

( $a_1$ – $a_4$  are constants) for analysis of anomalous SAXS (programs GAUSS2, LORQ1, LOREQ2, LOREQ3). Equation (10) was proposed by Koberstein *et al.*<sup>9</sup> and has been shown to model anomalous SAXS correctly<sup>9,10</sup>. For reasons outlined before, equation (10) was smeared according to equation (6) and fitted to the measured SAXS curves directly.

The first part of equation (10) represents the scattering due to long-range heterogeneities and the second part the additional contribution of the screened chains (compare equation (4)). The parameter  $a_4^{-1/2}$  in equation (10) should therefore be equal to the screening length  $\xi$  determined from Zimm plots. With variable parameters  $a_1$ – $a_4$  (equation (10)) one obtains good fits over the whole range of data (program LOREQ2) but  $a_4^{-1/2}$  deviates up to 15% from  $\xi$  determined from Zimm plots. These deviations arise because equation (4) or equation (10) respectively is no longer valid at large  $h$  values. In a refined approach the value of  $a_4$  (equation (10)) was fixed to  $a_4 = \xi^{-2}$  (Table 1) and fits were tried with a successively shortened set of data (say  $h_{\min}$  to  $h$  value no. 50,  $h_{\min}$  to  $h$  value no. 45, etc.) until a good match was obtained (program LOREQ3). Figure 7 shows an example of a fit obtained with program LOREQ3.

Generally all four smeared fits obtainable for one measured SAXS curve agree nearly exactly within the range of data. Owing to the missing information and inherent extrapolation in the models divergence in the range  $h < h_{\min}$  is large and calculated  $p(r)$  functions differ.

In Table 3 the averaged values of the four models for the radius of the long-range heterogeneities  $R_{\text{LRH}} = \langle R^2 \rangle^{1/2}$  (compare equation (5)) are listed. Error propagation based on statistical errors including covariances is carried out for all calculations but naturally falls short of the

Table 3

$M_w$ ( $\text{g mol}^{-1}$ )	$c$ ( $\text{g l}^{-1}$ )	$R_{\text{LRH}}$ (nm)
600 000	100.00	$30 \pm 33\%$
480 000	113.97	$40 \pm 14\%$
59 000 <sup>9</sup>	150.00	61
260 000	150.48	$43 \pm 30\%$
480 000	174.60	$45 \pm 46\%$
260 000	201.22	$54 \pm 34\%$
59 000 <sup>9</sup>	300.00	73

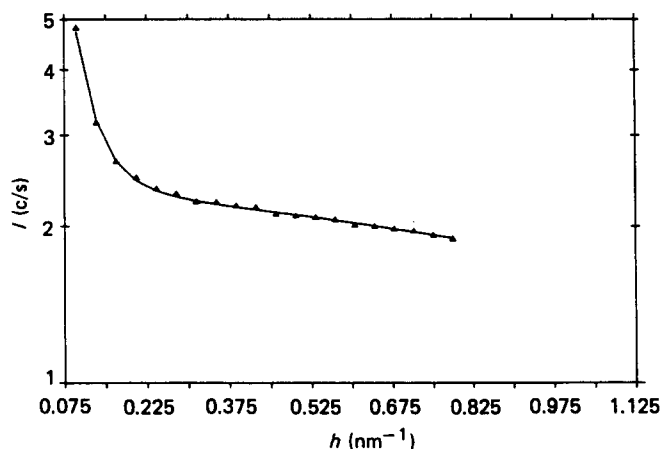


Figure 7 Smeared fit with program LOREQ3 to a smeared SAXS curve:  $\blacktriangle$ , measured data,  $h_{\min}$  to  $h$  value no.: —, fit. PS/BE,  $M_w = 480\,000\text{ g mol}^{-1}$ ,  $c = 174.6\text{ g l}^{-1}$ ,  $T = 21.0^\circ\text{C}$

deviations for  $R_{\text{LRH}}$  listed in Table 3. For comparison values obtained by Koberstein *et al.*<sup>9</sup> with small-angle neutron scattering (SANS) are included in Table 3. Though we could not detect anomalous SAXS in the polystyrene solution  $c = 199.3\text{ g l}^{-1}$ ,  $M_w = 52\,000\text{ g mol}^{-1}$ , Koberstein *et al.*<sup>9</sup> reported anomalous SANS for a polystyrene solution in benzene with a concentration of  $150\text{ g l}^{-1}$  and molecular weight of  $59\,000\text{ g mol}^{-1}$ .

Owing to large errors in  $R_{\text{LRH}}$  no conclusion about dependence on concentration or molecular weight can be drawn, yet. Nevertheless, the situation might become better with a larger amount of data.

A quantitative analysis of amount of anomalous SAXS, however, is only feasible with much better resolution.

## CONCLUSIONS

The screening length  $\xi$  calculated from Zimm plots of desmeared SAXS curves is in good agreement with the average length  $\langle L \rangle$  calculated with the IFT method via the  $p(r)$  function. Values calculated with the IFT method via the second moment of the  $p(r)$  functions show reasonable agreement, but deviate slightly. In all, the comparison demonstrates the reliability of the IFT for direct evaluation of slit length smeared SAXS curves.

The anomalous SAXS present in some SAXS curves at high concentrations is evaluated with the IFT method and a four-parameter random two-phase model. The size of the long-range heterogeneities responsible for anomalous SAXS is calculated. Owing to errors no systematic variation with concentration or molecular weight of polystyrene can be found. The size of the long-range heterogeneities agrees reasonably with values given by Koberstein *et al.*<sup>9</sup> for a sample of polystyrene ( $M_w = 59\,000\text{ g mol}^{-1}$ ) in benzene.

## ACKNOWLEDGEMENTS

This work was sponsored by the Deutsche Forschungsgemeinschaft and the Fonds der Chemischen Industrie, to whom we express our grateful thanks.

## REFERENCES

- 1 Guinier, A. and Fournet, G. 'Small-Angle Scattering of X-Rays', Wiley, New York, 1955
- 2 Glatter, O. and Kratky, O. 'Small Angle X-Ray Scattering', Academic Press, London and New York, 1982
- 3 de Gennes, P. G. 'Scaling Concepts in Polymer Physics', Cornell University Press, Ithaca, NY, 1979
- 4 Flory, P. J. 'Principles of Polymer Chemistry', Cornell University Press, Ithaca, NY, 1967
- 5 Daoud, M., Cotton, J. P., Farnoux, B., Jannink, G., Sarma, G., Benoit, H., Duplessix, R., Picot, C. and de Gennes, P. G. *Macromolecules* 1975, **8**, 804
- 6 Cotton, J. P., Farnoux, B. and Jannink, G. *J. Chem. Phys.* 1976, **65**, 1101
- 7 Okano, K., Wada, E., Kurita, K. and Fukuro, H. *J. Appl. Crystallogr.* 1978, **11**, 507
- 8 King, J. S., Boyer, W., Wignall, G. D. and Ullman, R. *Macromolecules* 1985, **18**, 709
- 9 Koberstein, J. T., Picot, C. and Benoit, H. *Polymer* 1985, **26**, 673
- 10 Gan, J. Y. S., Francois, J. and Guenet, J.-M. *Macromolecules* 1986, **19**, 173
- 11 Kube, O. Thesis 1985, Technische Universität Berlin, D83
- 12 Brown, W. and Johnsen, R. *Macromolecules* 1985, **18**, 379
- 13 Wenzel, M., Burchard, W. and Schätzel, K. *Polymer* 1986, **27**, 195
- 14 Kube, O. and Springer, J. *J. Appl. Crystallogr.* 1987, **20**, 41
- 15 Morton, M., Rembaum, A. A. and Hall, J. L. *J. Polym. Sci. A* 1963, **1**, 461
- 16 Wyman, D. P., Elyash, L. J. and Frazer, W. J. *J. Polym. Sci. A* 1965, **3**, 681
- 17 Bracewell, R. N. 'The Fourier Transform and its Applications', McGraw-Hill Kogakusha, London and Paris, 1978